Measurement of Thermodynamic Parameters for Hydrophobic Mismatch 2: Intermembrane Transfer of a Transmembrane Helix†

Yoshiaki Yano, Mai Ogura, and Katsumi Matsuzaki*

Graduate School of Pharmaceutical Sciences, Kyoto University, Sakyo-ku, Kyoto 606-8501, Japan

Received November 7, 2005; Revised Manuscript Received January 17, 2006

ABSTRACT: Hydrophobic matching between proteins and lipids is essential for the thermodynamic stability of integral membrane proteins. However, there is no direct thermodynamic information available about the intermembrane transfer of proteins between membranes with different hydrophobic thicknesses, which is crucial for understanding hydrophobic mismatch. This article reports the complete set of thermodynamic parameters (ΔG, ΔH, ΔS, and ΔC_p) for the intermembrane transfer of the inert hydrophobic model transmembrane helix NBD-$(AALALAA)_3$-NH_2 (NBD: 7-nitro-2-1,3-benzoxadiazol-4-yl), which is exchangeable between vesicles, from 1-palmitoyl-2-oleoyl-*sn*-glycero-3-phosphocholine (POPC) to dimonounsaturated-phosphocholine lipid bilayers with different hydrophobic thicknesses (C14−C22) at 37−58 °C. The transfer free energies were calculated from equilibrium values of the extent of helix transfer from donor to acceptor lipid vesicles, as monitored by a decrease in fluorescence resonance energy transfer from the NBD group to a lipid-labeled Rhodamine in the donor upon transfer to the quencher-free acceptor. Under hydrophobic mismatch conditions up to ∼7 Å, the helix partitioning became unfavorable up to +7 kJ mol^{-1}, hampered by an increase in entropic (up to +20 kJ mol^{-1}) and enthalpic (up to +66 kJ mol^{-1}) terms in thinner and thicker membranes, respectively. Together with the results that H/D exchange at the membrane interface was accelerated in thinner membranes the obtained thermodynamic parameters were reasonably explained assuming that hydrophobic mismatch induces aqueous exposure or membrane burial of the helix termini, resulting in excess energies originating from the hydration of terminal hydrophobic residues or the unfavorable Born energy of terminal partial charges of the helix macrodipole.

Geometric matching between the hydrophobic parts of integral membrane proteins and the hydrophobic thickness of surrounding lipid bilayers have been considered to be important parameters for membrane−protein interactions (*1*−*4*). Membrane proteins, such as Ca^{2+} ATPase (*5*) and diacylglycerol kinase (*6*), show maximal activity in membranes with C16−C18 fatty acyl chains. In addition to the regulation of activities of membrane proteins, an essential role of hydrophobic mismatch in mammalian cells is the sorting of membrane proteins in the exocytotic pathway in which membrane thickness increases from Golgi to plasma membranes (*7*, *8*). Because a statistical analysis shows that thinner Golgi membranes and thicker plasma membranes preferentially include transmembrane helices of ∼15 and ∼20 hydrophobic residues, respectively (*8*), the proteins are considered to be sorted, at least partly, driven by hydrophobic matching. Because the distinct lipid compositions of Golgi (relatively rich in glycerolipids) and plasma membranes (rich in cholesterol and sphingolipids) are maintained by vesicular transport between them, membrane-lateral segregation with different hydrophobic thicknesses should occur in the vesicle formation process, although information on this mechanism is still rather limited (*9*). In this process, membrane proteins also should be localized in hydrophobically matched membranes by lateral partitioning, although differences in other physicochemical properties between lipid domains might also affect protein partitioning. Consistent with the idea mentioned above, lengthening of the hydrophobic parts of Golgi membrane proteins results in their sorting to plasma membranes (*9*). Inversely, shortening of the hydrophobic parts of plasma membrane proteins causes their retention in the Golgi apparatus (*9*). Interestingly, Engelman's group recently demonstrated that the situation is more complex, with proteins and lipids not necessarily hydrophobically matched in some biological membranes (*10*).

A thermodynamic model postulated by Mouritsen and Bloom in 1984 (mattress model) assumes that under hydrophobic mismatch conditions the balance between excess energies originating from the deformation of the lipids surrounding the proteins and the exposure of the hydrophobic parts of the proteins (under positive mismatch) or lipids (under negative mismatch) to water determines the response to hydrophobic mismatch (*4*), although in most cases, elastic deformation of lipids has been attributed to a major response to the avoidance of highly unfavorable aqueous exposure of hydrophobic groups. However, as the authors pointed out, the interaction parameters introduced in the model need to be refined with further experimental support. Although this model has been successfully used to explain the effects of protein inclusions on membrane-phase-transition tempera-

† Supported in part by Grant-in-Aid for JSPS Fellows (155377) from the Ministry of Education, Culture, Sports, Science and Technology of Japan.

* To whom correspondence should be addressed. E-mail: katsumim@pharm.kyoto-u.ac.jp. Tel: 81-75-753-4574. Fax: 81-75-761-2698.

10.1021/bi052286w CCC: $33.50
Published on Web 02/17/2006

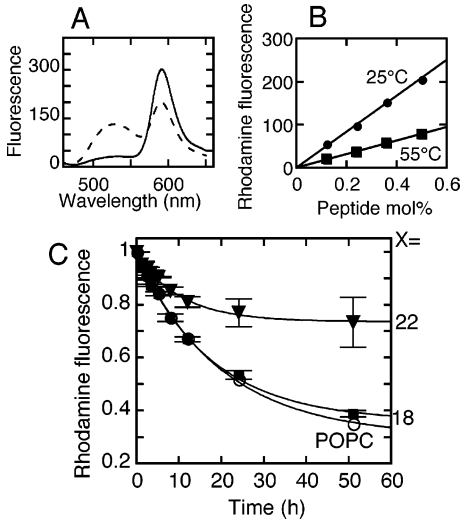

FIGURE 1: Measurement of the intervesicular transfer of the peptide. (A) Representative emission spectral change upon intervesicular transfer of **I**. Donor POPC vesicles containing 0.5 mol % **I** and 2 mol % Rh-PE were incubated with acceptor diC (18:1) PC vesicles at a donor-to-acceptor lipid ratio of 1:5 (total lipid concentrations, 1.2 mM). NBD and rhodamine emission maxima are around 530 and 590 nm, respectively. Emission spectra before (—) and after (- - -) 66 h of incubation are shown. (B) Sensitized rhodamine fluorescence intensity at 590 nm is proportional to the amount of peptides in the donor vesicles. The background contribution from directly excited Rh-PE fluorescence has been subtracted. (C) Time course of sensitized rhodamine fluorescence intensity in the presence of acceptor POPC (○), diC (18:1) PC (■), and diC (22:1) PC (▼) vesicles at 37 °C ($n = 2$). The observed values are fitted by the single-exponential function $F_x(t) = F_x(\infty) + (F_x(0) - F_x(\infty))\exp(-kt)$.

tures (*2*), there are few studies that directly measure the thermodynamic parameters (Gibbs free energy change ΔG, enthalpy change ΔH, entropy change ΔS, and heat-capacity change ΔC_p) for membrane partitioning of proteins under hydrophobic mismatch conditions.

Instead of membrane proteins, model transmembrane helices as basic folding units of helical membrane proteins have been widely used to elucidate the driving forces of membrane protein folding and the consequences of hydrophobic mismatch (*11*−*15*). Several studies using model transmembrane helices reported that hydrophobic mismatch actually decreases the partitioning of the helix (*12*, *16*−*18*), although the correspondence to thermodynamic parameters have not been measured. In these studies, the helix−lipid interaction was evaluated on the basis of the degree of peptide incorporation into the membranes in the sample preparation (*12*, *17*) and the partitioning between the membrane surface (noninserted) and transmembrane configurations (*16*, *18*). However, the effects of hydrophobic mismatch on the membrane partitioning of the helix can be evaluated directly by the helix-intermembrane-transfer process via the aqueous phase ((*19*), also see Figure 1 in the preceding article).

In this article, the complete set of thermodynamic parameters for the intermembrane transfer of the inert hydrophobic model transmembrane helix NBD-(AALALAA)$_3$-NH$_2$ (NBD: 7-nitro-2-1,3-benzoxadiazol-4-yl)[1] (**I**) between membranes with different hydrophobic thicknesses was determined. The peptide is convenient for measuring the intermembrane-transfer process because it does not contain anchoring, charged residues at the ends. The thermodynamic parameters suggest that the helix partitioning into both thinner and thicker membranes was energetically unfavorable because of exposure and membrane burial of helix termini, respectively. The water accessibility of the helix termini at the membrane−water interface, as examined by H/D exchange, also supported this conclusion. The origins of unfavorable energies under hydrophobic mismatch conditions will be discussed. Together with the results of the preceding article, the importance of electrostatic energy at the water−membrane interface is highlighted.

MATERIALS AND METHODS

Materials. NBD-(AALALAA)$_3$-NH$_2$ (**I**) was custom synthesized and characterized by the Peptide Institute (Minoh, Japan). The purity of the peptide (> 90%) was confirmed by reverse-phase high-performance liquid chromatography, amino acid analysis and ion-spray mass spectroscopy. To generate hydrophobic mismatch, doubly monounsaturated phosphocholines with 14 to 22 acyl chain carbons were used: 1,2-dimyristoleoyl-*sn*-glycero-3-phosphocholine, 1,2-dipalmitoleoyl-*sn*-glycero-3-phosphocholine, 1,2-dioleoyl-*sn*-glycero-3-phosphocholine, 1,2-dieicosenoyl-*sn*-glycero-3-phosphocholine, and 1,2-dierucoyl-*sn*-glycero-3-phosphocholine (abbreviated as diC (*X*:1) PCs, $X = 14$, 16, 18, 20, and 22, respectively). Hydrophobic thicknesses of diC (*X*:1) PCs were estimated assuming a linear relationship between the thickness and the number of acyl chain carbons: diC (14:1) PC, 20 Å; diC (16:1) PC, 23.5 Å; diC (18:1) PC, 27Å; diC (20:1) PC, 30.5 Å; and diC (22:1) PC, 34 Å (*20*). All lipids were purchased from Avanti Polar Lipids (Alabaster, AL). Spectrograde chloroform and methanol were products of Nacalai Tesque (Kyoto, Japan). *N*-(6-tetramethylrhodaminethiocarbamoyl)-1,2-dihexadecanol-*sn*-glycero-3-phosphoethanolamine, triethylammonium salt (TR-PE) and Lissamine Rhodamine B 1,2-dihexadecanol-*sn*-glycero-3-phosphoethanolamine, triethylammonium salt (Rh-PE) were obtained from Molecular Probes (Eugene, OR). The lipids and the peptides were dissolved in chloroform and methanol, respectively. The lipid concentration was determined in triplicate by phosphorus analysis (21). The concentration of the dye-labeled peptide was determined on the basis of the extinction coefficient in methanol ($\epsilon_{449} = 20\,000\ M^{-1}$), which was obtained from absorbance measurements combined with a quantitative analysis of amino acids performed in duplicate.

Preparation of Vesicles. Large unilamellar vesicles (LUVs) were prepared by an extrusion method (*22*) using a buffer containing 10 mM Tris, 150 mM NaCl, and 1mM EDTA (pH 7.4). Freezing and thawing of multilamellar vesicles containing peptides was avoided.

[1] Abbreviations: diC (14:1) PC, 1,2-dimyristoleoyl-*sn*-glycero-3-phosphocholine; diC (16:1) PC, 1,2-dipalmitoleoyl-*sn*-glycero-3-phosphocholine; diC (18:1) PC, 1,2-dioleoyl-*sn*-glycero-3-phosphocholine; diC (20:1) PC, 1,2-dieicosenoyl-*sn*-glycero-3-phosphocholine; diC (22:1) PC, 1,2-dierucoyl-*sn*-glycero-3-phosphocholine; ESI, electrospray ionization; FRET, fluorescence resonance energy transfer; LUVs, large unilamellar vesicles; NBD, 7-nitro-2-1,3-benzoxadiazol-4-yl; POPC, 1-palmitoyl-2-oleoyl-*sn*-glycero-3-phosphocholine; Rh-PE, lissamine rhodamine B 1,2-dihexadecanol-*sn*-glycero-3-phosphoethanolamine, triethylammonium salt; TR-PE, *N*-(6-tetramethylrhodaminethiocarbamoyl)-1,2-dihexadecanol-*sn*-glycero-3-phosphoethanolamine, triethylammonium salt.

Intervesicular Transfer of Peptide. Donor POPC LUVs (200 μM) incorporating 0.5 mol % **I** and 2 mol % Rh-PE as an NBD quencher were mixed with an excess of acceptor LUVs (1 mM) composed of diC (*X*:1) PCs. Fluorescence emission spectra between 430 and 650 nm (excited at 450 nm) were measured on a Shimadzu RF-5300 spectrofluorometer. The efficiency of peptide transfer to acceptor-vesicle populations was determined by a decrease in sensitized fluorescence of Rh-PE at 590 nm ($n = 2$). After subtracting the contribution of directly excited Rh-PE fluorescence, the intensity of the sensitized fluorescence of Rh-PE was obtained from a least-squares curve fitting using a linear combination of the emission spectra of **I** and Rh-PE. The vesicles containing peptide **I** did not show any fusion or exchange of lipids (TR-PE and Rh-PE) between donor and acceptor vesicles for at least 50 h (data not shown).

Electrospray Ionization (ESI) Mass Spectrometry. LUVs composed of diC (*X*:1) PCs incorporating 2 mol % **I** were prepared in 10 mM ammonium acetate buffer (pH 7.4). H/D exchange was initiated by diluting the LUVs 30-fold in deuterated ammonium acetate buffer at 25 °C ($n = 3$). ESI mass measurements were performed on an Applied Biosystems Mariner electrospray time-of-flight mass instrument (Foster City, CA) operating in the positive ion mode. In LUVs dispersed in the H_2O buffer, the peptide was detected as singly charged $[M + H]^+$ ($m/z = 1925.3$) and $[M + Na]^+$ ($m/z = 1947.3$) ions as well as doubly charged ions. In this study, the spectrometer's variables were optimized to detect singly charged proton adducts of the peptide used for the evaluation of the H/D exchange. The sample solution was introduced into the spectrometer at a flow rate of 2 μL/min using a syringe pump with a stainless steel needle, ~5 mm from the orifice. The electrospray needle, nozzle, and skimmer voltages were set at +2900 V, +150 V, and +11 V, respectively. The flow rate of the curtain nitrogen gas to assist solvent vaporization was 0.6 L/min. The nozzle and quadrupole temperatures were fixed at 150 and 140 °C, respectively.

RESULTS

Helix Partitioning between Membranes. The absence of charged residues and the moderate hydrophobicity of **I** enable us to measure the membrane insertion/dissociation processes of the helix. The helix-transfer free energies (ΔG_t) between the different membranes were measured on the basis of the finding that the helix slowly transfers between lipid bilayers via the aqueous phase (*19*). In the donor vesicles composed of POPC labeled with 2 mol % Rh-PE, FRET from the NBD moiety of **I** to Rh-PE occurred strongly, whereas in the acceptor vesicles without the quencher, FRET was relieved (Figure 1A). The FRET signals were detected as sensitized fluorescence of Rh-PE instead of the donor NBD fluorescence because the emission-quantum yield and spectral shape of NBD depend on the lipid species in the acceptor vesicles. The sensitized fluorescence intensity of Rh-PE was confirmed to be proportional to the peptide concentration in the donor vesicles (Figure 1B). Therefore, if $F_X(t)$ is the sensitized rhodamine fluorescence at time *t* after mixing with acceptor vesicles composed of diC (*X*:1) PC, the amounts of the peptide in the donor and the acceptor vesicles are simply proportional to $F_X(t)$ and $F_X(0) - F_X(t)$, respectively, because the fraction of the peptide in the aqueous phase is negligible. $F_x(t)$ followed the first-order kinetics with a limiting value $F_x(\infty)$ (Figure 1C), which was dependent on the acceptor lipid species. The equilibrium peptide concentrations in the donor ($[P]_D$) and the acceptor ($[P]_A$) vesicles can be calculated as

$$[P]_D(t) = \frac{F_X(\infty)}{F_X(0)} \cdot [P]_0 \quad (1)$$

$$[P]_A = \frac{F_X(0) - F_X(\infty)}{F_X(0)} \cdot \frac{[L]_D}{[L]_A}[P]_D \quad (2)$$

$[P]_0$ and $([L]_D/[L]_A)$ represent the initial concentration of the helix in the donor vesicles and the donor-to-acceptor lipid concentration ratio, respectively. Our previous studies have suggested that in both the donor and acceptor vesicles a fraction of the helices also exists as an antiparallel dimer depending on peptide concentration and lipid composition, although the helix dissociates from membranes as a monomer (*19*). The concentration of monomers in each membrane [M] was calculated from total peptide concentration [P] and the monomer-dimer association constant K_a obtained in the preceding paper

$$[M] = \frac{\sqrt{8K_a[P] + 1} - 1}{4K_a} \quad (3)$$

$[M]_A/[M]_D$ gives the partition coefficient of the helix monomer from the donor to the acceptor. Although the monomer fraction was significantly dependent on acceptor membranes (e.g., ~0.9 and ~0.5 in diC (14:1) PC and diC (22:1) PC, respectively), there were no notable differences between ΔG_t values calculated from [M] and those calculated from [P] because in equilibrium, the monomer fraction in the donor became similar to that in the acceptor (within ±0.15). To precisely determine the partition coefficient of the peptide between diC (*X*:1) PC and POPC, $K_{t(monomer)}^{POPC \rightarrow X}$, we also used pure POPC vesicles as the acceptor vesicles in each experiment, to obtain $[M]_{POPC}$ values.

$$K_{t(monomer)}^{POPC \rightarrow X} = \frac{[M]_X}{[M]_{POPC}} \quad (4)$$

The free energy of transfer of the monomer from POPC to diC (*X*:1) PC was calculated as

$$\Delta G_{t(monomer)}^{POPC \rightarrow X} = -RT \ln K_{t(monomer)}^{POPC \rightarrow X} \quad (5)$$

The corresponding ΔG_t values for the helix dimer were determined by

$$\Delta G_{t(dimer)}^{POPC \rightarrow X} = -\Delta G_a^{POPC} + 2\Delta G_{t(monomer)}^{POPC \rightarrow X} + \Delta G_a^X \quad (6)$$

ΔG_a^{POPC} and ΔG_a^X denote the Gibbs free energy values for antiparallel dimer formation in POPC and diC (*X*:1) PC, respectively. The latter values were reported in the preceding paper. ΔG_a^{POPC}, ΔH_a^{POPC}, and $-T\Delta S_a^{POPC}$ values obtained using methods similar to those in the preceding paper were -12.8 ± 0.2, -27.9 ± 1.6, and $+15.1 \pm 1.6$ kJ mol^{-1} (at 308 K), respectively, assuming $\Delta C_{p(a)} = 0$. Figure 2A and B summarize $\Delta G_{t(monomer)}^{POPC \rightarrow X}$ and $\Delta G_{t(dimer)}^{POPC \rightarrow X}/2$ values at 37, 44,

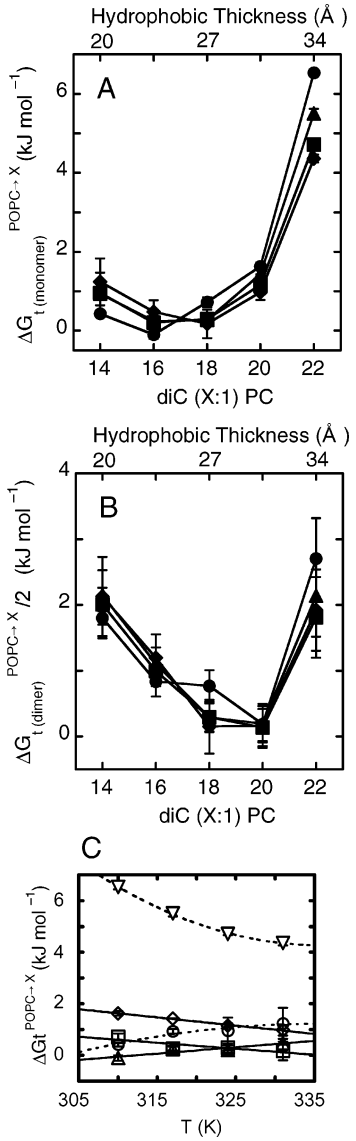

FIGURE 2: Thermodynamics of helix transfer. (A) $\Delta G_{t\,(monomer)}^{POPC\rightarrow X}$ values for **I** from POPC to diC (*X*:1) PCs at 37 (●), 44 (▲), 51 (■), and 58 °C (♦). (B) $\Delta G_{t\,(dimer)}^{POPC\rightarrow X}/2$ values for **I** from POPC to diC (*X*:1) PCs at 37 (●), 44 (▲), 51 (■), and 58 °C (♦). (C) van't Hoff plot of $\Delta G_{t\,(monomer)}^{POPC\rightarrow X}$ in the range of 37−58 °C. Symbols: X = 14 (○), 16 (△), 18 (□), 20 (◇), and 22 (▽).

51, and 58 °C. DiC (16:1) PC (at 37 °C) and diC (18:1) PC (at 44, 51, and 58 °C) showed the smallest $\Delta G_{t(monomer)}^{POPC\rightarrow X}$ values (<1 kJ mol^{-1}), and both thinner and thicker membranes gave larger values up to 7 kJ mol^{-1}, demonstrating that hydrophobic mismatch decreases helix partitioning. Notably, helix transfer into thicker membranes was significantly unfavorable. Although the end-to-end length of the helix is 31.5 Å assuming a canonical α-helical structure, the average hydrophobic length based on the geometrical configuration of hydrophobic amino acids (*23*) is 2−3 residues shorter (27−28.5 Å), similar to or slightly longer than the hydrophobic thickness of diC (18:1) PC membranes (*20*). However, the helix dimer preferentially partitioned in thicker membranes with the smallest $\Delta G_{t(dimer)}^{POPC\rightarrow X}$ values in diC (18:1) PC (at 44, 51, and 58 °C) and diC (20:1) PC (at 37 °C) membranes.

The temperature dependence of ΔG_t was analyzed assuming a constant $\Delta C_{p(t)}$ in the temperature range studied (*24*).

$$\Delta G_t = \Delta H_t + \Delta C_{p(t)}(T - T_{ref}) - T\Delta S_t - T\Delta C_{p(t)} \ln\left(\frac{T}{T_{ref}}\right) \quad (7)$$

T and T_{ref} represent the observed temperature and the standard-state reference temperature (308 K in this study), respectively. As in the analysis for helix-antiparallel-dimer formation (in the preceding paper), the data was adequately fitted by linear regression (Figure 2C, solid lines) in the cases where X = 16, 18, and 20, indicating that the changes in enthalpy and entropy upon dimerization are almost constant ($\Delta C_{p\,(t)} \approx 0$), whereas obvious deviations from linearity were observed for X = 14 and 22. The obtained thermodynamic parameters ΔH_t, $-T\Delta S_t$, and $\Delta C_{p(t)}$ at 308 K are summarized in Table 1. In thinner membranes, the unfavorable free energies originated from an increase in the entropic term $-T\Delta S_t$ (up to +20 kJ mol^{-1}), whereas in thicker membranes, an increase in the enthalpic term ΔH_t (up to +66 kJ mol^{-1}) hampered membrane partitioning. Corresponding thermodynamic parameters for helix dimer transfer were similarly calculated (Table 2). A similar tendency was observed for dimer transfer, although a significant decrease in the unfavorable enthalpic term in thicker membranes (+41 kJ mol^{-1} for diC (22:1) PC) was observed.

ESI Mass Spectrometry. To further support the interpretation of the above thermodynamic data, the effects of hydrophobic thickness on the accessibility of water molecules to the main-chain amide protons of the helix were examined using the H/D exchange reaction. Recent studies have demonstrated that the H/D exchange efficiency of transmembrane helices at the water−membrane interface in LUV suspensions can be measured by ESI mass spectrometry (*25*−*27*). Because membranes are sufficiently permeable to water (*28*), we assumed that the helix termini on the outer and inner leaflets of LUVs were equally exposed to deuterium after the dilution of LUV suspensions with a deuterated buffer. Figure 3 shows the average mass after the H/D exchange in diC (*X*:1) PCs for the singly charged deuterium adducts. The measurements were performed 10−20 min after dilution to detect the numbers of amino protons that quickly exchanged with deuterium under hydrophobic mismatch conditions. After this fast exchange, the average mass did not increase significantly, at least until 60 min (data not shown). We focus on the differences in the average mass of the peptide among various diC (*X*:1) PCs to evaluate the degree of accessibility of water instead of the overall mass increase, which may involve H/D exchange in the ionization process via collisions with gaseous deuterium molecules. In thinner diC (14:1) PC and diC (16:1) PC, significantly larger mass values were observed, suggesting that the helix termini protrude into the aqueous phase. However, the helix in diC (18:1) PC and thicker PCs exhibited similar degrees of H/D exchange. Because an effective H/D exchange should occur only in a sufficiently polar environment in which the helix can relax to form H bonds with water, the above results indicate that as membrane thickness increases the helix termini are positioned in similar, more hydrophobic environments.

DISCUSSION

Adaptation to Hydrophobic Mismatch. The results obtained using Fourier transform infrared polarized spectroscopy in

Table 1: Thermodynamic Parameters for Helix Monomer Transfer from POPC to diC (*X*:1) PC at 308 K

membranes	$\Delta G_{t\,(monomer)}$ (kJ mol^{-1})	$\Delta H_{t\,(monomer)}$ (kJ mol^{-1})	$-T\Delta S_{t\,(monomer)}$ (kJ mol^{-1})	$\Delta C_{p\,(t)\,(monomer)}$ (kJ K^{-1} mol^{-1})	R^2
diC (*X*:1) PC					
14[a]	+0.3 ± 0.1	−19.8 ± 3.9	+20.1 ± 3.9	+0.8 ± 1.1	0.92
14[b]	+0.4 ± 0.1	−10.4 ± 2.9	+10.9 ± 2.9		0.88
16[b]	−0.1 ± 0.1	−7.7 ± 2.3	+7.6 ± 2.3		0.86
18[b]	+0.7 ± 0.1	+7.8 ± 3.2	−7.1 ± 3.2		0.73
20[b]	+1.7 ± 0.1	+11.5 ± 0.5	−9.8 ± 0.5		0.99
22[a]	+6.9 ± 0.1	+65.9 ± 3.9	−59.0 ± 3.8	−2.2 ± 0.3	0.99
22[b]	+6.6 ± 0.1	+38.7 ± 4.9	−32.1 ± 4.9		0.96

[a] Estimated assuming that $\Delta C_{p(t)}$ is constant in the temperature range (eq 7). [b] Estimated assuming $\Delta C_{p(t)} = 0$.

Table 2: Thermodynamic Parameters for Helix Dimer Transfer from POPC to diC (*X*:1) PC at 308 K

membranes	$\Delta G_{t\,(dimer)}/2$ (kJ mol^{-1})	$\Delta H_{t\,(dimer)}/2$ (kJ mol^{-1})	$-T\Delta S_{t\,(dimer)}/2$ (kJ mol^{-1})	$\Delta C_{p\,(t)\,(dimer)}/2$ (kJ K^{-1} mol^{-1})
diC (*X*:1) PC				
14[a]	+1.7 ± 0.1	−14.7 ± 2.4	+16.4 ± 2.4	+0.5 ± 0.6
14[b]	+1.9 ± 0.1	−4.1 ± 2.4	+4.3 ± 1.4	
16[b]	+1.0 ± 0.4	−5.8 ± 1.6	+6.8 ± 1.5	
18[b]	+0.7 ± 0.4	+6.1 ± 1.9	−5.3 ± 1.8	
20[b]	+0.7 ± 0.5	−3.8 ± 1.6	+4.5 ± 1.6	
22[a]	+3.3 ± 1.2	+40.5 ± 6.8	−37.2 ± 6.7	−0.9 ± 1.1
22[b]	+2.6 ± 1.2	+12.6 ± 10.5	−34.5 ± 2.6	

[a] Estimated assuming that $\Delta C_{p(t)}$ is constant in the temperature range. [b] Estimated assuming $\Delta C_{p(t)} = 0$.

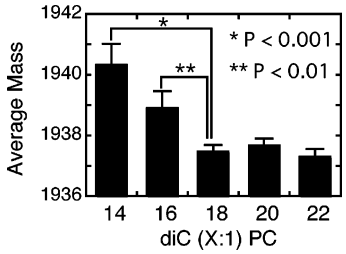

FIGURE 3: Average masses of singly charged deuterium adducts of **I** after a 10 min H/D exchange in diC (*X*:1) PCs ($n = 3$). LUVs composed of diC (*X*:1) PCs incorporating 2 mol % **I** were prepared in 10 mM ammonium acetate buffer (pH 7.4). H/D exchange was initiated by diluting LUVs 30-fold in a deuterated ammonium acetate buffer (10 mM ammonium acetate, pD 7.4) at 25 °C.

the preceding paper and H/D exchange-ESI mass spectrometry in the present study reveal the way helices and lipids adapt to hydrophobic mismatch. As discussed in the preceding paper, changes in structure and orientation of the helix and the deformation of the membranes are not major adaptations to the mismatch, suggesting that the dielectric environments around the helix termini can significantly change. Consistent with this notion, the H/D exchange experiments demonstrated that the accessibility of water molecules to the helix backbone was actually increased in thinner membranes (positive mismatch). The mass increase may not quantitatively indicate the water-exposed length of the helix because (1) H/D exchange requires the unwinding of the helix, which does not necessarily accompany complete aqueous exposure of the helix and (2) the background H/D exchange in the ionization process apparently reduces the mass difference before an analysis. Despite these limitations, the observed ~3 Da difference between diC (14:1) PC and diC (18:1) PC suggests a protrusion of ~4.5 Å of the helix termini into water in diC (14:1) PC (assuming a helix length of 1.5 Å per backbone amide), corresponding to ~65% of the difference in hydrophobic thickness between these bilayers (~7 Å). These results support a model in which exposure/burial of the helix termini are major adaptations to the mismatch. It should be noted that the polarity around the helix termini in which the degree of H/D exchange alters significantly (C14−C16, $\epsilon > 30$) is higher than the polarity range in which the transfer free energy (mainly Born energy) changes dramatically (C20−C22, $\epsilon < 30$).

Thermodynamic Parameters for Monomer Transfer. The above exposure/burial of the helix termini model was assumed in the following estimations of the unfavorable energies for the partition of the helix into thinner or thicker membranes. The burial of the helix termini into more hydrophobic environments results in an increase in the enthalpic Born energy in thicker membranes. When the relative dielectric constant changes from ϵ_1 to ϵ_2, the difference in Born energy is calculated as

$$\Delta\mu_{\epsilon_1\rightarrow\epsilon_2} = \frac{2z^2e^2N_A}{8\pi\epsilon_0 a}\left(\frac{1}{\epsilon_2} - \frac{1}{\epsilon_1}\right) \quad (8)$$

z and a express the charge and the radius of the ion, respectively. N_A denotes the Avogadro number. Partial charges originating from the helix macrodipole ($|z| = 0.5$) are assumed to localize at the terminal atoms with $a = 1.4$ Å. Following the discussion in the preceding paper, the dielectric constant around the helix termini should decrease from 45 (in diC (14:1) PC) to 9.5 (in diC (20:1) PC), corresponding to an increase in Born energy by 21 kJ mol^{-1}. This value is about two-thirds of the observed difference in $\Delta H_{t(monomer)}$ (+31 kJ mol^{-1}). The remaining 10 kJ mol^{-1} may arise from a decrease in enthalpy in thinner membranes because of the exposure of terminal residues to the aqueous phase (up to 15 kJ mol^{-1}, see below). As discussed in the preceding paper, the $\Delta\Delta H^{14\rightarrow 22}{}_{H-H}$ value was significantly affected by the partial aqueous exposure of the terminal NBD and DABMI groups upon dimerization. Therefore, the dielectric constant around the helix termini in diC (22:1) PC was estimated geometrically ($\epsilon \sim 4$, see the preceding paper).

The calculated Born transfer energy assuming $\epsilon = 4$ (+57 kJ mol^{-1}) well explains the $\Delta\Delta H^{14\rightarrow 22}{}_{t\,(monomer)}$ value (+86 kJ mol^{-1}). The difference may originate from the burial of the hydrophobic residues and the NBD group into the hydrophobic core (see below).

ΔC_p is considered to be the hallmark of the hydrophobic effect instead of ΔS. From the helix transfer from POPC to thinner diC (14:1) PC, $\Delta C_{p(t)(monomer)}$ was positive (+0.8 kJ K^{-1} mol^{-1}), indicating a decrease in hydrophobic interaction. In a study of the membrane partitioning of Cox IVp peptides, the transfer of Ala and Leu side chains from the aqueous phase to the membrane surface was reported to yield ΔC_p values of −0.05 and −0.38 kJ K^{-1} mol^{-1}, respectively (*24*). Thus, the observed $\Delta C_{p(t)}$ value is reasonably explained by the exposure of terminal residues such as four Ala and two Leu residues (+1.0 kJ K^{-1} mol^{-1}). The increase in the entropic term should originate from a change in the hydrophobic interaction near the helix termini. Hydrophobic interaction is mainly entropic but also has a minor enthalpic effect. The transfer of Leu and Ala side chains from the membrane interface to the aqueous phase yields $\Delta H = -2.8$ and −2.4 kJ mol^{-1} and $-T\Delta S = +14$ and +6 kJ mol^{-1}, respectively (*24*). The exposure of two Leu and four Ala residues to the aqueous phase is estimated to induce a decrease in the enthalpic term by ∼15 kJ mol^{-1} and an increase in the entropic term by ∼52 kJ mol^{-1}. The latter value is comparable to the observed value for the transfer from diC (20:1) PC to a thinner diC (14:1) PC membrane (+30 kJ mol^{-1}). Note that this estimation does not include the contribution of the peptide backbone, which may significantly affect the partitioning energetics (*29*). The changes in the lipid−lipid interactions between the two types of membranes also contribute to the observed thermodynamic parameters. The observed large $\Delta C_{p(t)}$ and ΔS_t values in diC (22:1) PC may be understood on the basis of the loss of hydrogen bonds upon the burial of the NBD group, in addition to the increased hydrophobic interaction.

Monomer versus Dimer. The most important difference between the helix monomer and the antiparallel dimer affecting membrane partitioning is considered to be the effective charges at the helix termini. In the dimer, partial charges originating from the helix macrodipole are partly neutralized by antiparallel association, resulting in a significant decrease in unfavorable Born energies upon transfer to thicker membranes (e.g., from +66 to +41 kJ mol^{-1} for diC (22:1) PC). Together with a marked increase in the entropic term (from −59 to −37 kJ mol^{-1} for diC (22:1) PC) that mostly compensates for the decrease in the enthalpic term, the free energy of the dimer transfer was more favorable by ∼3 kJ mol^{-1} than that of the monomer. However, upon transfer to thinner membranes, a helix−helix contact in the dimer reduced the unfavorable aqueous exposure of the hydrophobic parts of the helix, resulting in a decrease in the entropic term (from +20 to +16 kJ mol^{-1} for diC (14:1) PC) and the ΔC_p term (from +0.8 to +0.5 kJ K^{-1} mol^{-1}).

Importance of Electrostatic Energy at the Water−Membrane Interface. According to the conventional view of hydrophobic mismatch, the primary principle to reduce the free energy of the system is assumed to satisfy maximal hydrophobic interaction, mainly by the deformation of flexible membranes (*1*). In addition to the principle, this series of articles concerning the first detailed thermodynamic analysis of self-association and membrane partitioning of the inert transmembrane helix under conditions of hydrophobic mismatch demonstrated that (1) bilayer deformation was not necessarily the major adaptation to the mismatch, and importantly (2) that there is another response to the mismatch other than satisfying maximal hydrophobic interaction: a change in electrostatic energy at the water−membrane interface (Figure 4). Partial charges at the helix termini originating from the helix macrodipole play a critical role in electrostatic energy. The electrostatic effects become prominent in thicker membranes (under negative mismatch conditions) because the polarity around the helix termini decreases as the hydrophobic thickness of the surrounding bilayers increases. The stronger helix dipole−dipole attraction drives antiparallel dimer formation, whereas the unfavorable Born energy significantly decreases helix partitioning. However, in thinner membranes, the hydration of terminal hydrophobic residues appears to modulate helix association and membrane partitioning, although the effects might be weaker than those of the electrostatic energy for the helix used in this study. These alterations in electrostatic energies as well as in hydrophobic energies under conditions of hydrophobic mismatch will become a basis for understanding the sorting of membrane proteins in the exocytotic pathway and the structural and functional modulation of protein activities by membrane thickness.

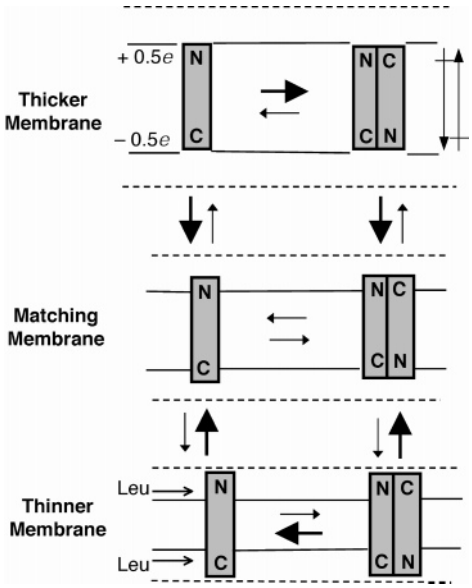

FIGURE 4: The exposure/burial of the helix termini model for hydrophobic mismatch. The origins of unfavorable partitioning energies are different in thinner and thicker membranes. In thinner membranes, the exposure of hydrophobic residues, especially Leu residues, to the aqueous environment causes a decrease in hydrophobic interaction (i.e., an increase in $\Delta C_{p(t)}$ and a decrease in entropy), whereas in thicker membranes, the burial of the helix termini into a more hydrophobic environment results in an increase in the enthalpic Born energy. The balance of these contributions determines the matching membrane thickness. In contrast, stronger attractions between helix macrodipoles in thicker membranes originate from the smaller dielectric environments of the helix terminus.

REFERENCES

1. de Planque, M. R. R., and Killian, J. A. (2003) Protein−lipid interactions studied with designed transmembrane peptides: role

of hydrophobic matching and interfacial anchoring, *Mol. Membr. Biol. 20*, 271−284.
2. Dumas, F., Lebrun, M. C., and Tocanne, J. F. (1999) Is the protein/lipid hydrophobic matching principle relevant to membrane organization and functions?, *FEBS Lett. 458*, 271−277.
3. Killian, J. A. (1998) Hydrophobic mismatch between proteins and lipids in membranes, *Biochim. Biophys.* Acta *1376*, 401−415.
4. Mouritsen, O. G., and Bloom, M. (1984) Mattress model of lipid−protein interactions in membranes, *Biophys. J. 46*, 141−153.
5. Lee, A. G. (2003) Lipid−protein interactions in biological membranes: a structural perspective, *Biochim.* Biophys. Acta *1612*, 1−40.
6. Pilot, J. D., East, J. M., and Lee, A. G. (2001) Effects of bilayer thickness on the activity of diacylglycerol kinase of *Escherichia coli*, *Biochemistry 40*, 8188−8195.
7. Munro, S. (1998) Localization of proteins to the Golgi apparatus, *Trends Cell Biol. 8*, 11−15.
8. Bretscher, M. S., and Munro, S. (1993) Cholesterol and the Golgi apparatus, *Science 261*, 1280−1281.
9. Holthuis, J. C., van Meer, G., and Huitema, K. (2003) Lipid microdomains, lipid translocation and the organization of intracellular membrane transport, *Mol. Membr. Biol. 20*, 231−241.
10. Mitra, K., Ubarretxena-Belandia, I., Taguchi, T., Warren, G., and Engelman, D. M. (2004) Modulation of the bilayer thickness of exocytic pathway membranes by membrane proteins rather than cholesterol, *Proc. Natl. Acad. Sci. U.S.A. 101*, 4083−4088.
11. Yano, Y., Takemoto, T., Kobayashi, S., Yasui, H., Sakurai, H., Ohashi, W., Niwa, M., Futaki, S., Sugiura, Y., and Matsuzaki, K. (2002) Topological stability and self-association of a completely hydrophobic model transmembrane helix in lipid bilayers, *Biochemistry 41*, 3073−3080.
12. de Planque, M. R. R., Goormaghtigh, E., Greathouse, D. V., Koeppe, R. E., II, Kruijtzer, J. A., Liskamp, R. M. J., de Kruijff, B., and Killian, J. A. (2001) Sensitivity of single membrane-spanning α-helical peptides to hydrophobic mismatch with a lipid bilayer: effects on backbone structure, orientation, and extent of membrane incorporation, *Biochemistry 40*, 5000−5010.
13. Mall, S., Broadbridge, R., Sharma, R. P., East, J. M., and Lee, A. G. (2001) Self-association of model transmembrane α-helices is modulated by lipid structure, *Biochemistry 40*, 12379−12386.
14. Choma, C., Gratkowski, H., Lear, J. D., and DeGrado, W. F. (2000) Asparagine-mediated self-association of a model transmembrane helix, *Nat. Struct. Biol. 7*, 161−166.
15. Zhou, F. X., Cocco, M. J., Russ, W. P., Brunger, A. T., and Engelman, D. M. (2000) Interhelical hydrogen bonding drives strong interactions in membrane proteins, *Nat. Struct. Biol. 7*, 154−160.
16. Ridder, A. N., van de Hoef, W., Stam, J., Kuhn, A., de Kruijff, B., and Killian, J. A. (2002) Importance of hydrophobic matching for spontaneous insertion of a single-spanning membrane protein, *Biochemistry 41*, 4946−4952.
17. Webb, R. J., East, J. M., Sharma, R. P., and Lee, A. G. (1998) Hydrophobic mismatch and the incorporation of peptides into lipid bilayers: a possible mechanism for retention in the Golgi, *Biochemistry 37*, 673−679.
18. Ren, J., Lew, S., Wang, Z., and London, E. (1997) Transmembrane orientation of hydrophobic α-helices is regulated both by the relationship of helix length to bilayer thickness and by the cholesterol concentration, *Biochemistry 36*, 10213−10220.
19. Yano, Y., and Matsuzaki, K. (2002) Membrane insertion and dissociation processes of a model transmembrane helix, *Biochemistry 41*, 12407−12413.
20. Lewis, B. A., and Engelman, D. M. (1983) Lipid bilayer thickness varies linearly with acyl chain length in fluid phosphatidylcholine vesicles, *J. Mol. Biol. 166*, 211−217.
21. Bartlett, G. R. (1959) Phosphorus assay in column chromatography, *J. Biol. Chem. 234*, 466−468.
22. Matsuzaki, K., Murase, O., Fujii, N., and Miyajima, K. (1996) An antimicrobial peptide, magainin 2, induced rapid flip-flop of phospholipids coupled with pore formation and peptide translocation, *Biochemistry 35*, 11361−11368.
23. Zhang, Y.-P., Lewis, R. N., Hodges, R. S., and McElhaney, R. N. (1992) Interaction of a peptide model of a hydrophobic transmembrane α-helical segment of a membrane protein with phosphatidylcholine bilayers: differential scanning calorimetric and FTIR spectroscopic studies, *Biochemistry 31*, 11579−11588.
24. Russell, C. J., Thorgeirsson, T. E., and Shin, Y. K. (1996) Temperature dependence of polypeptide partitioning between water and phospholipid bilayers, *Biochemistry 35*, 9526−9532.
25. Hansen, R. K., Broadhurst, R. W., Skelton, P. C., and Arkin, I. T. (2002) Hydrogen/deuterium exchange of hydrophobic peptides in model membranes by electrospray ionization mass spectrometry, *J. Am. Soc. Mass Spectrom. 13*, 1376−1387.
26. Demmers, J. A., van Duijn, E., Haverkamp, J., Greathouse, D. V., Koeppe, R. E., II, Heck, A. J., and Killian, J. A. (2001) Interfacial positioning and stability of transmembrane peptides in lipid bilayers studied by combining hydrogen/deuterium exchange and mass spectrometry, *J. Biol. Chem. 276*, 34501−34508.
27. Demmers, J. A., Haverkamp, J., Heck, A. J., Koeppe, R. E., II, and Killian, J. A. (2000) Electrospray ionization mass spectrometry as a tool to analyze hydrogen/deuterium exchange kinetics of transmembrane peptides in lipid bilayers, *Proc. Natl. Acad. Sci. U.S.A. 97*, 3189−3194.
28. Fettiplace, R., and Haydon, D. A. (1980) Water permeability of lipid membranes, *Physiol. Rev. 60*, 510−550.
29. Jayasinghe, S., Hristova, K., and White, S. H. (2001) Energetics, stability, and prediction of transmembrane helices, *J. Mol. Biol. 312*, 927−934.

BI052286W